Supplementary information

Differential binding of auto-antibodies to MOG isoforms in inflammatory demyelinating diseases

Kathrin Schanda[1], MSc, Patrick Peschl[1], PhD, Magdalena Lerch[1], MSc, Barbara Seebacher[1], PhD, Swantje Mindorf[2], MSc, Nora Ritter[2], MSc, Monika Probst[3], PhD, Harald Hegen[1], MD, PhD, Franziska Di Pauli[1], MD, PhD, Eva-Maria Wendel[4], MD, Christian Lechner[5], MD, Matthias Baumann[5], MD, Sara Mariotto[6], MD PhD, Sergio Ferrari[6], MD, Albert Saiz[7], MD, PhD, Michael Farrell[8], MD, Maria Isabel Leite[9], MD, DPhil, Sarosh R. Irani[9], MD, DPhil, Jacqueline Palace[9], FRCP, DM, Andreas Lutterotti[10], MD, Tania Kümpfel[11], MD, Sandra Vukusic[12], MD, Romain Marignier[12], MD, PhD, Patrick Waters[9], PhD, Kevin Rostasy[13], MD, Thomas Berger[14], MD, Christian Probst[2], PhD, Romana Höftberger[15], MD, Markus Reindl[1#], PhD

[1] Clinical Department of Neurology, Medical University of Innsbruck, Innsbruck, Austria

[2] Euroimmun Medizinische Labordiagnostika AG, Lübeck, Germany

[3] Institute for Quality Assurance (ifQ) affiliated to Euroimmun, Lübeck, Germany

[4] Department of Pediatrics, Olgahospital/Klinikum Stuttgart, Stuttgart, Germany

[5] Department of Pediatrics I, Medical University of Innsbruck, Innsbruck, Austria

[6] Neurology Unit, Department of Neuroscience, Biomedicine, and Movement Sciences, University of Verona, Verona, Italy

[7] Neuroimmunology and Multiple Sclerosis Unit, Service of Neurology, Hospital Clinic, Institut d'Investigacions Biomèdiques August Pi i Sunyer (IDIBAPS), Universitat de Barcelona, Barcelona, Spain

[8] Beaumont Hospital, Dublin, Ireland

[9] Oxford Autoimmune Neurology Group, Nuffield Department of Clinical Neurosciences, University of Oxford, Oxford, UK

[10] Neuroimmunology and MS Research, Department of Neurology, University Hospital Zurich & University of Zurich, Switzerland

[11] Institute of Clinical Neuroimmunology, Biomedical Center and University Hospital, Ludwig-Maximilians University, Munich, Germany

[12] Department of Neurology, Hospices civils de Lyon, Hôpital neurologique Pierre Wertheimer, Lyon, France

[13] Paediatric Neurology, Witten/Herdecke University, Children's Hospital Datteln, Datteln, Germany

[14] Department of Neurology, Medical University of Vienna, Vienna, Austria

[15] Division of Neuropathology and Neurochemistry, Department of Neurology, Medical University of Vienna, Vienna, Austria

Corresponding author

1. Supplementary methods

Table e-1 Demographic and clinical data of patients and controls according to their MOG-IgG serostatus

	MOG-IgG negative (176)	**MOG-IgG positive (202)**
MOG-IgG titer [a]	0 (0-20)	640 (320-1280)
Neuropathological investigation	0	6 [1-5]
Females	92/147 (63%) [h]	100/202 (49%)
Age (years) [a]	36.2 (18.2-45.6)	19.0 (7.2-42.3)
Children (<18 years)	35/176 (20%)	96/202 (47%)
Disease duration (years) [a]	1.5 (0.0-3.6)	0.1 (0.0 to 1.84)
Diagnosis [b]		
Non-MS [c]	23/176 (13%)	191/202 (95%)
MS	56/176 (32%)	8/202 (4%)
HC	97/176 (55%)	3/202 (1%)
Clinical phenotype [b,c]		
Cerebral [d]	13/23 (57%)	58/191 (30%)
Opticospinal [e]	10/23 (43%)	122/191 (64%)
Mixed [f]	0/23 (0%)	11/191 (6%)
Disease course [c,g]		
Monophasic	20/23 (87%)	103/191 (54%)
Recurrent	3/23 (13%)	88/191 (46%)

[a] median with interquartile range; [b] at the time sample was taken; [c] demyelinating non-MS phenotype consistent with MOG-IgG associated disease (MOGAD); [d] ADEM (54), MDEM (14), brainstem syndrome (2), encephalitis (1); [e] optic neuritis (74), myelitis (21), optic neuritis and myelitis (3), NMOSD (34); [f] ADEMON (3) or opticospinal with cerebral symptoms (8); [g] at last follow-up available; [h] information not available from 29 HC (blood donors).
HC healthy control, MS multiple sclerosis, non-MS demyelinating non-MS disease.

Cloning of human MOG isoforms

Three human MOG isoform expression vector plasmids were created by site-directed mutagenesis (Quick Change II mutagenesis Kit, Promega) using the pEGFP-N1-hMOGα1 plasmid as matrix. In a first step, the hMOGβ1 isoform was cloned to create the unique 3` sequence of all beta isoforms. Thereafter, isoforms hMOGα2 and hMOGβ2 were cloned from hMOG alpha1 or hMOGβ1, respectively. The genes for hMOGα3 and hMOGβ3 were obtained from GenScript and subcloned into the pEGFP-N1 expression vectors using restriction sites EcoRI/XhoI. All genes were sequenced and proved correct to the consensus sequence except for the presence of A520G in the hMOGα1 precursor transcript variant and thereof derived isoform transcript variants (α2, β1, β2), causing a missense mutation 174 I [ATC] >V [GTC]. However, a search in the SNP library revealed this mutation to be a natural variant (NCBI SNB rs3130253) representing 93-100% of the human population. Therefore, a correction to the consensus sequence was deemed unnecessary. Controls were created by insertion of three STOP codons at the 3‘ terminus of the respective pEGFP-N1 isoform/species plasmid via mutagenesis and removal of the EGFP tag by restriction enzyme digestion. These plasmids coded for the native, untagged proteins.

Human MOGα1 mutants

All mutations were created by site-directed mutagenesis of the pEGFP-N1-hMOGα1 plasmid. The selection of human MOG mutants used in this study was based on previous reports from the literature (see references below in Table e-2) or differences between human MOG and mouse/rat MOG within the extracellular domain and expected loop structures thereof (figure e-1).

Table e-2 Human MOGα1 mutants analyzed in this study

Mutation	Reason for selection and impact
N31Q	glycosylation site removed/no glycosylation [6-10]
P42S	mouse/rat specific, major epitope of human MOG-IgG [6-9]
E64K	possible micro motif for C1q binding [11, 12]
A75S	rat specific [6, 7]
R86Q	mouse/rat specific [6, 7]
H103A+S104E	abolishes binding of monoclonal anti-MOG 8-18-C5 [6-9]

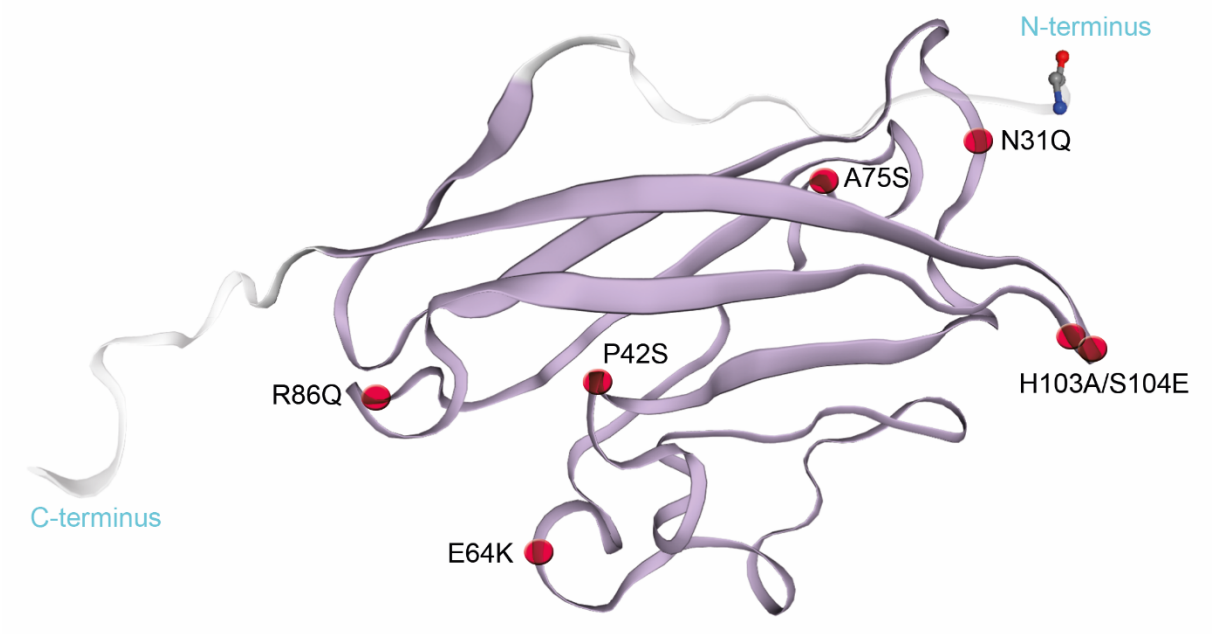

Figure e-1 Modified schematic of the human MOG extracellular domain (amino acids) 30-153 and location of mutations (the immunoglobulin V-set domain is marked in purple); modelling was done with SWISS-MODEL Workspace **(**Waterhouse et al 2018, SWISS-MODEL: homology modelling of protein structures and complexes [13]; Guex et al 2009: Automated comparative protein structure modeling with SWISS-MODEL and Swiss-PdbViewer: A historical perspective [14]). This protein model generated by SWISS-MODEL is licensed under the CC BY-SA 4.0 Creative Commons Attribution-ShareAlike 4.0 International License (https://swissmodel.expasy.org/docs/terms_of_use).

Gentle fixation protocol for surface staining (figure e-2)

96 well plates with transfected cells were removed from the incubator 24h after transfection and left for 10min at room temperature. Supernatant was removed, followed by fixation (4% methanolfree PFA/5% sucrose in PBS) for 5min. Fixant was completely removed and cells were washed two times with PBS, followed by blocking with 5% milkpowder in PBS for 1 hour. Blocking was removed and monoclonal rh8-18-C5 antibody (1µg/ml) was added in 5% BSA-PBS for 30min at room temperature. Cells were washed 2 times with 1% BSA-PBS and the secondary antibody (anti-human IgG Fc-specific, Alexa 594 conjugated; 1:750) was added in 5% BSA-PBS for 30min at room temperature. Cells were washed again with 1% BSA-PBS and images were taken. Live cell staining as depicted in Figures 2 and 5 of the main manuscript was performed in parallel on the same day according to published protocols [15].

Surface live cell based assay FACS (CBA-FACS) staining of HEK cells expressing MOG isoforms (figure e-3)

The goal of this representative CBA-FACS staining was to show the surface staining of all six MOG isoforms with a different method to the life CBA-IF performed in this study. Briefly, a six well plate was seeded with HEK293 cells and 24h later transfected with the respective MOG isoform plasmid (hMOGα1, hMOGα2, hMOGα3, hMOGβ1, hMOGβ2, hMOGβ3). After 24h, cells were harvested, counted, adjusted to a concentration of 0,2 Mio/100µl buffer (10% FCS in 1mM EDTA-PBS) and recovered with slow rotation at room temperature for 30min. After recovery, cells were seeded into a 96 well round-bottom plate and either buffer only or first antibody (recombinant humanized monoclonal antibody 8-18-C5 [16, 17], 1µg/ml) was added and the plate was incubated at 4°C for 1h. After two washing steps, secondary antibody (Dianova, anti-human IgG Fc-specific, APC-conjugated, 1:200) was added to all wells for 30min at room temperature, followed by two final washing steps. Cells were resuspended in 100µl buffer and analyzed using the Accuri C6 FlowCytometer (BD Biosciences), gating on the whole HEK population with a limit of 50.000 cells.

2. Supplementary results

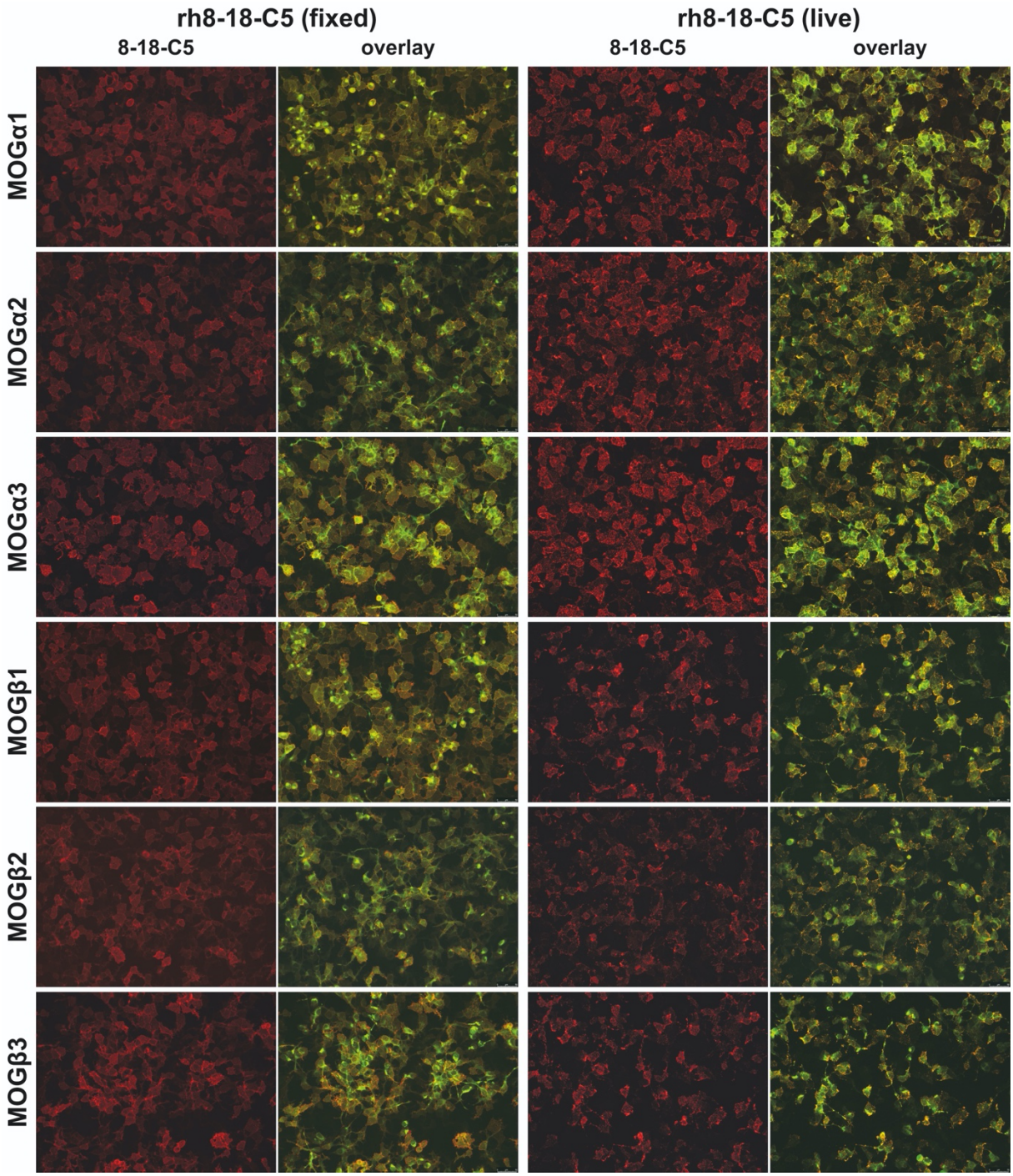

Figure e-2 Expression of MOG isoforms α1, α2, α3, β1, β2 and β3 in HEK293 cells Binding of humanized recombinant monoclonal antibody rh8-18-C5 to paraformaldehyde fixed, non-permeabilized cells (fixed CBA-IF) and living cells (live CBA-IF). The fixed CBA-IF shows a mostly smooth, specific surface staining of all isoforms compared to the patchier surface staining observed in live CBA-IF due to antibody crosslinking and membrane dynamics during the staining process. Only specific antibody (red) and overlay images

(MOG-transfected cells are shown in green) were used to reduce image size (20 x magnification).

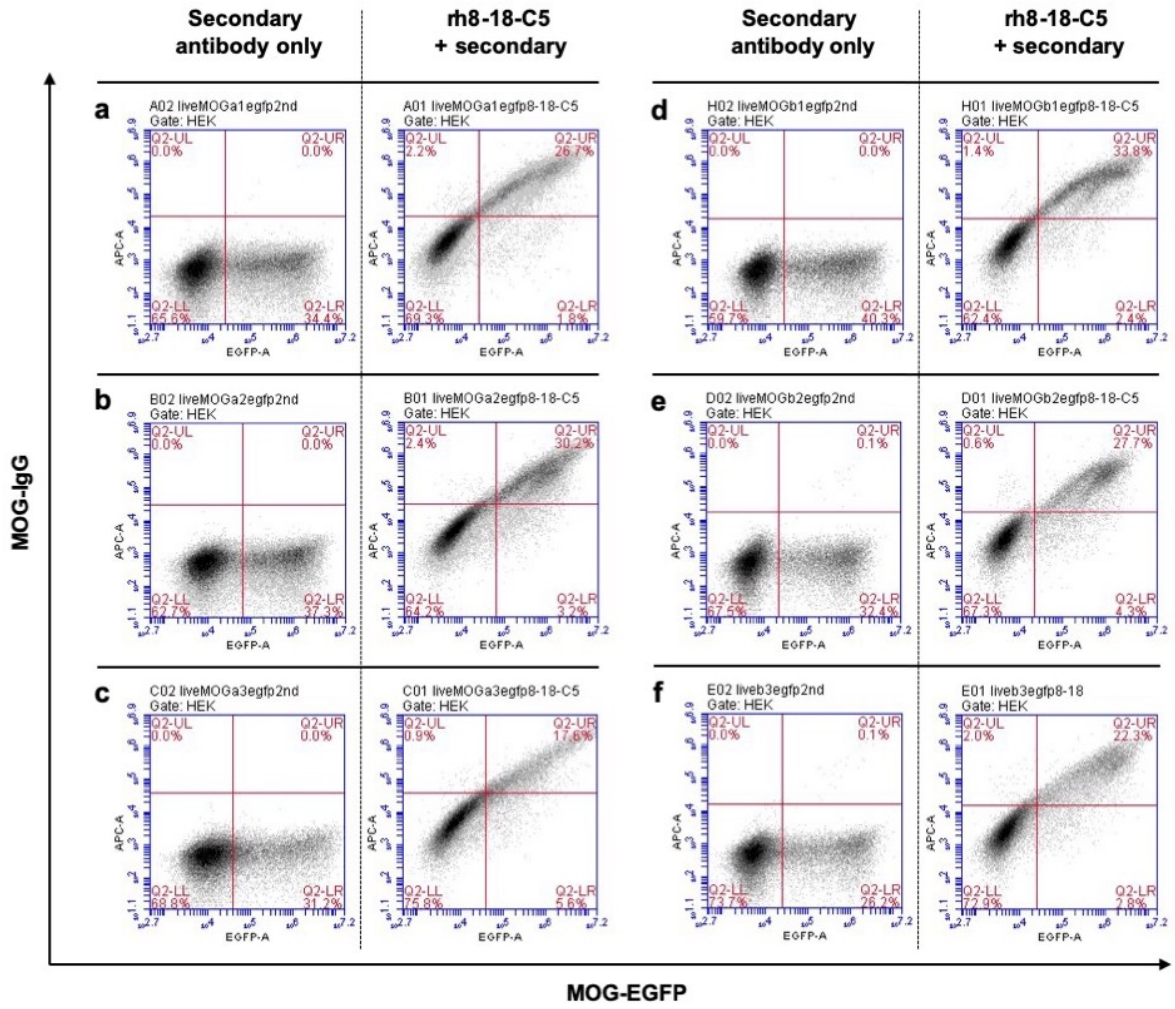

Figure e-3 Live CBA-FACS surface staining of HEK cells transiently transfected with different human MOG isoforms (EGFP-A, MOG-EGFP) showing specific surface staining of the monoclonal anti-MOG rh8-18-C5 antibody (APC-A, MOG-IgG): (a) hMOGα1, (b) hMOGα2, (c) hMOGα3, (d) hMOGβ1, (e) hMOGβ2, (f) hMOGβ3. Cells were stained with recombinant humanized monoclonal antibody 8-18-C5 or the secondary anti-human IgG(Fc) antibody as control.

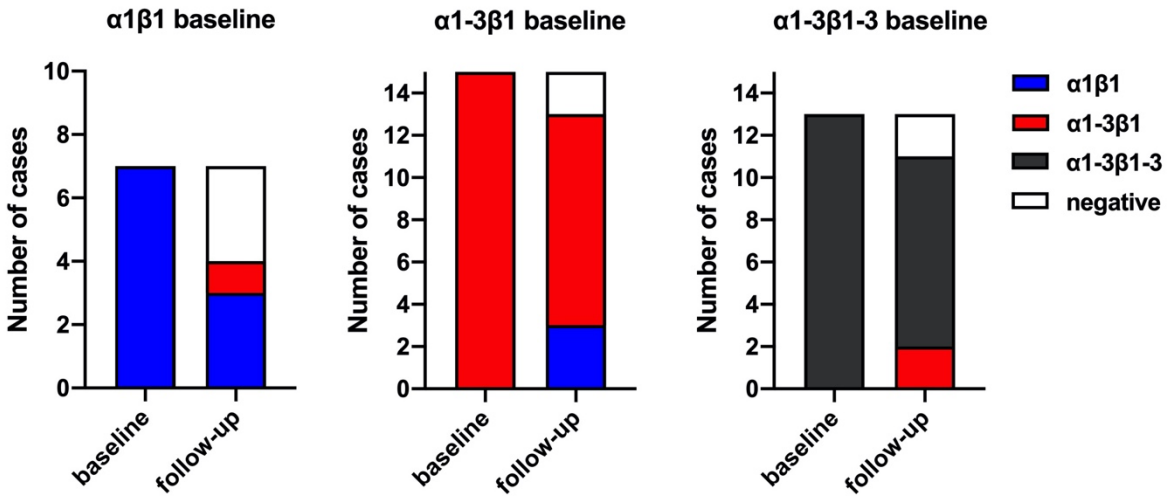

Figure e-4 Results of follow-up samples from 34 individuals (7 α1β1, 15 α1-3β1 and 13 α1-3β1-3) according to the three MOG isoform binding patterns at baseline and at last follow-up (median observation period of 4.1 years, range 0.8-12.1 years). Three of the 7 (43%) patients with α1β1, 10 of the 15 (71%) patients with α1-3β1 and 9 of the 13 (69%) patients with α1-3β1-3 binding patterns kept their isoform binding pattern. The other patients converted to α1-3β1 (3), α1β1 (3) or became seronegative (7). There was no conversion from α1β1 to α1-3β1-3 or vice versa.

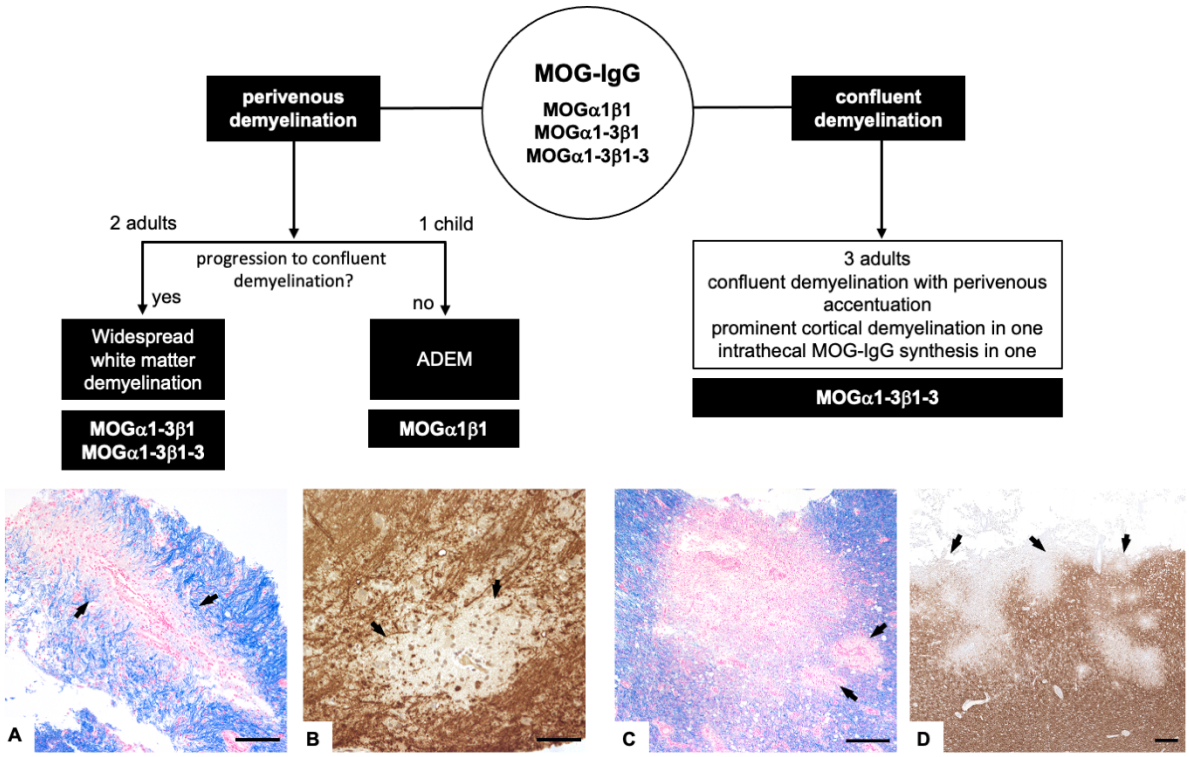

Figure e-5 MOG isoform binding patterns in 6 cases with available neuropathological assessment (recently published as case reports [1-4] and/or included in a series of patients, to describe the pathology of CNS demyelination accompanied by MOG-IgG [5]). At disease/relapse onset, neuropathological features of patients with different MOG isoform binding patterns can be divided into two groups: 1) patients with perivenous demyelination. **A** biopsy of an adult patient (MOG α1-3β1 binding pattern, Luxol fast blue staining) and **B** biopsy of a child (*MOG α1β1* binding pattern, myelin basic protein staining). Progression from perivenous to confluent demyelination in later disease stages of group 1 was variable, ranging from widespread white matter demyelination with perivenous accentuation to monophasic disease course without progression. 2) patients presenting with confluent demyelination: the recognition of all 6 MOG isoforms (MOG α1-3β1-3 binding pattern) in these patients was associated with plaque-like demyelination with perivenous accentuation **(C**, Luxol fast blue staining**)**. Moreover, one patient showed prominent cortical demyelination **(D,** myelin basic protein staining**)** and another intrathecal antibody synthesis. Arrows in **A**, **B**, and **C** indicate perivenous accentuation of demyelination; arrows in **D** indicate cortical demyelination. Scale bars: **A** 100µm, **B** 50µm, **C** 250µm, **D** 500µm.

Table e-3 Frequency of MOG-IgG positive cases and positive and negative predictive values according to MOG-IgG isoform titers

cut-off	MOG-α1	MOG-α2	MOG-α3	MOG-β1	MOG-β2	MOG-β3
≥ 1:20						
Non-MS	202/214 94.4%	100/214 46.7%	129/214 60.3%	202/214 94.4%	56/214 26.2%	76/214 35.5%
MS	24/64 37.5%	7/64 10.9%	17/64 26.6%	25/64 39.1%	2/64 3.1%	6/64 9.4%
HC	32/100 32.0%	5/100 5.0%	25/100 25.0%	32/100 32.0%	2/100 2.0%	7/100 7.0%
PPV	78.3%	89.3%	75.4%	78.0%	93.3%	85.4%
NPV	90.0%	57.1%	58.9%	89.9%	50.3%	52.2%
≥ 1:40						
Non-MS	200/214 93.5%	86/214 40.2%	115/214 53.7%	198/214 92.5%	52/214 24.3%	66/214 30.8%
MS	16/64 25.0%	2/64 3.1%	5/64 7.8%	15/64 23.4%	1/64 1.6%	3/64 4.7%
HC	12/100 12.0%	3/100 3.0%	8/100 8.0%	11/100 11.0%	1/100 1.0%	2/100 2.0%
PPV	87.7%	94.5%	89.8%	88.4%	96.3%	93.0%
NPV	90.7%	55.4%	60.4%	89.6%	50.0%	51.8%
≥ 1:80						
Non-MS	193/214 90.2%	68/214 31.8%	97/214 45.3%	191/214 89.3%	47/214 22.0%	58/214 27.1%
MS	11/64 17.2%	2/64 3.1%	2/64 3.1%	11/64 17.2%	1/64 1.6%	1/64 1.6%
HC	3/100 3.0%	2/100 2.0%	4/100 4.0%	4/100 4.0%	0/100 0.0%	1/100 1.0%
PPV	93.2%	94.4%	94.2%	92.7%	97.9%	96.7%
NPV	87.7%	52.3%	57.5%	86.6%	49.44%	50.9%
≥ 1:160						
Non-MS	190/214 88.8%	53/214 24.8%	89/214 41.6%	185/214 86.4%	36/214 16.8%	47/214 22.0%
MS	8/64 12.5%	1/64 1.6%	1/64 1.6%	8/64 12.5%	0/64 0.0%	0/64 0.0%
HC	3/100	0/100	3/100	2/100	0/100	0/100

	3.0%	0.0%	3%	2.0%	0.0%	0.0%
PPV	94.5%	98.1%	95.7%	94.9%	100.0%	100.0%
NPV	86.4%	50.3%	56.1%	84.2%	48.0%	49.5%
≥ 1:320						
Non-MS	166/214 77.6%	44/214 20.6%	66/214 30.8%	164/214 76.6%	22/214 10.3%	37/214 17.3%
MS	4/64 6.3%	0/64 0.0%	0/64 0.0%	3/64 4.7%%	0/64 0.0%	0/64 0.0%
HC	2/100 2.0%	0/100 0.0%	1/100 1.0%	0/100 0.0%	0/100 0.0%	0/100 0.0%
PPV	96.5%	100.0%	98.5%	98.2%	100.0%	100.0%
NPV	76.7%	49.1%	52.4%	76.3%	46.1%	48.1%
≥ 1:640						
Non-MS	128/214 59.8%	32/214 15.0%	52/214 24.3%	121/214 56.5%	13/214 6.1%	20/214 9.3%
MS	0/64 0.0%	0/64 0.0%	0/64 0.0%	1/64 1.6%	0/64 0.0%	0/64 0.0%
HC	0/100 0.0%	0/100 0.0%	0/100 0.0%	0/100 0.0%	0/100 0.0%	0/100 0.0%
PPV	100.0%	100.0%	100.0%	99.2%	100.0%	100.0%
NPV	65.6%	47.4%	50.3%	63.7%	44.9%	45.8%
≥ 1:1280						
Non-MS	89/214 41.6%	16/214 7.5%	36/214 16.8%	82/214 38.3%	7/214 3.3%	11/214 5.1%
MS	0/64 0.0%	0/64 0.0%	0/64 0.0%	0/64 0.0%	0/64 0.0%	0/64 0.0%
HC	0/100 0.0%	0/100 0.0%	0/100 0.0%	0/100 0.0%	0/100 0.0%	0/100 0.0%
PPV	100.0%	100.0%	100.0%	100.0%	100.0%	100.0%
NPV	56.7%	45.3%	48.0%	55.4%	44.2%	44.7%
≥ 1:2560						
Non-MS	46/214 21.5%	3/214 1.4%	20/214 9.3%	45/214 21.0%	0/214 0.0%	3/214 1.4%
MS	0/64 0.0%	0/64 0.0%	0/64 0.0%	0/64 0.0%	0/64 0.0%	0/64 0.0%
HC	0/100	0/100	0/100	0/100	0/100	0/100

	0.0%	0.0%	0.0%	0.0%	0.0%	0.0%
PPV	100.0%	100.0%	100.0%	100.0%		100.0%
NPV	49.4%	43.7%	45.8%	49.2%		43.7%
≥ 1:5120						
Non-MS	20/214 9.3%	0/214 0.0%	8/214 3.7%	23/214 10.7%	0/214 0.0%	1/214 0.5%
MS	0/64 0.0%	0/64 0.0%	0/64 0.0%	0/64 0.0%	0/64 0.0%	0/64 0.0%
HC	0/100 0.0%	0/100 0.0%	0/100 0.0%	0/100 0.0%	0/100 0.0%	0/100 0.0%
PPV	100.0%		100.0%	100.0%		100.0%
NPV	45.8%		44.3%	46.2%		43.5%

PPV: positive predictive value for MOG-IgG associated with a non-MS (MOGAD) clinical presentation (true positive); NPV: negative predictive value for MOG-IgG negative controls (MS or HC; true negative).

Table e-4 Association of individual MOG isoform antibody titers with predominant clinical phenotypes in patients with non-MS demyelinating disease

	Cerebral (n=71)	**Opticospinal (n=132)**	**Mixed (n=11)**
MOGα1 (1:) [a] ≥ 1:160	640 (160-2560) 58 (81.7%)	640 (320-1280) 122 (92.4%)	1280 (1280-2560) 11 (100%)
MOGα2 (1:) [a] ≥ 1:40	0 (0-80) 29 (40.8%)	0 (0-160) 52 (39.4%)	40 (0-320) 7 (63.6%)
MOGα3 (1:) [a] ≥ 1:160	40 (0-320) 31 (43.7%)	40 (0-320) 50 (37.9%)	160 (40-1280) 8 (72.7%)
MOGβ1 (1:) [a] ≥ 1:160	640 (160-2560) 57 (80.3%)	640 (320-1280) 117 (88.6%)	1280 (1280-2560) 11 (100%)
MOGβ2 (1:) [a] ≥ 1:40	0 (0-0) 16 (22.5%)	0 (0-20) 31 (23.5%)	0 (0-80) 5 (45.5%)
MOGβ3 (1:) [a] ≥ 1:80	0 (0-40) 17 (23.9%)	0 (0-80) 36 (27.3%)	0 (0-160) 5 (45.5%)

[a] median with 25th-75th percentiles

Table e-5 Association of individual MOG isoform antibody titers with disease course at last follow-up in patients with non-MS demyelinating disease

	Monophasic (n=123)	**Recurrent (n=91)**
MOGα1 (1:) [a] ≥ 1:160	640 (160-1280) 103 (83.7%)	640 (320-1280) 88 (96.7%)
MOGα2 (1:) [a] ≥ 1:40	0 (0-80) 49 (39.8%)	20 (0-160) 39 (42.9%)
MOGα3 (1:) [a] ≥ 1:160	40 (0-320) 46 (37.4%)	40 (0-640) 43 (47.3%)
MOGβ1 (1:) [a] ≥ 1:160	640 (160-1280) 99 (80.5%)	640 (320-1280) 86 (94.5%)
MOGβ2 (1:) [a] ≥ 1:40	0 (0-20) 29 (23.6%)	0 (0-20) 23 (25.3%)
MOGβ3 (1:) [a] ≥ 1:80	0 (0-80) 32 (26.0%)	0 (0-80) 26 (28.6%)

[a] median with 25th-75th percentiles

3. Supplementary References

1. Hochmeister S, Gattringer T, Asslaber M, et al. A Fulminant Case of Demyelinating Encephalitis With Extensive Cortical Involvement Associated With Anti-MOG Antibodies. Front Neurol 2020;11:31.

2. Di Pauli F, Hoftberger R, Reindl M, et al. Fulminant demyelinating encephalomyelitis: Insights from antibody studies and neuropathology. Neurology(R) neuroimmunology & neuroinflammation 2015;2:e175.

3. Kortvelyessy P, Breu M, Pawlitzki M, et al. ADEM-like presentation, anti-MOG antibodies, and MS pathology: TWO case reports. Neurology(R) neuroimmunology & neuroinflammation 2017;4:e335.

4. Lang J, Biebl A, Gruber A, et al. Teaching Case 5-2018: Integrated morphological and immunological work-up of neurosurgical specimen allows accurate diagnosis of neuroinflammatory lesions: an example of acute disseminated encephalomyelitis (ADEM) associated with anti-MOG antibodies. Clin Neuropathol 2018;37:206-208.

5. Hoftberger R, Guo Y, Flanagan EP, et al. The pathology of central nervous system inflammatory demyelinating disease accompanying myelin oligodendrocyte glycoprotein autoantibody. Acta Neuropathol 2020;139:875-892.

6. Breithaupt C, Schubart A, Zander H, et al. Structural insights into the antigenicity of myelin oligodendrocyte glycoprotein. Proceedings of the National Academy of Sciences of the United States of America 2003;100:9446-9451.

7. Mayer MC, Breithaupt C, Reindl M, et al. Distinction and temporal stability of conformational epitopes on myelin oligodendrocyte glycoprotein recognized by patients with different inflammatory central nervous system diseases. J Immunol 2013;191:3594-3604.

8. Spadaro M, Winklmeier S, Beltran E, et al. Pathogenicity of human antibodies against myelin oligodendrocyte glycoprotein. Ann Neurol 2018;84:315-328.

9. Tea F, Lopez JA, Ramanathan S, et al. Characterization of the human myelin oligodendrocyte glycoprotein antibody response in demyelination. Acta neuropathologica communications 2019;7:145.

10. Marti Fernandez I, Macrini C, Krumbholz M, et al. The Glycosylation Site of Myelin Oligodendrocyte Glycoprotein Affects Autoantibody Recognition in a Large Proportion of Patients. Front Immunol 2019;10:1189.

11. Johns TG, Bernard CC. Binding of complement component Clq to myelin oligodendrocyte glycoprotein: a novel mechanism for regulating CNS inflammation. Molecular immunology 1997;34:33-38.

12. Clements CS, Reid HH, Beddoe T, et al. The crystal structure of myelin oligodendrocyte glycoprotein, a key autoantigen in multiple sclerosis. Proceedings of the National Academy of Sciences of the United States of America 2003;100:11059-11064.

13. Waterhouse A, Bertoni M, Bienert S, et al. SWISS-MODEL: homology modelling of protein structures and complexes. Nucleic Acids Res 2018;46:W296-W303.
14. Guex N, Peitsch MC, Schwede T. Automated comparative protein structure modeling with SWISS-MODEL and Swiss-PdbViewer: a historical perspective. Electrophoresis 2009;30 Suppl 1:S162-173.
15. Reindl M, Schanda K, Woodhall M, et al. International multicenter examination of MOG antibody assays. Neurology(R) neuroimmunology & neuroinflammation 2020;7.
16. Linington C, Bradl M, Lassmann H, Brunner C, Vass K. Augmentation of demyelination in rat acute allergic encephalomyelitis by circulating mouse monoclonal antibodies directed against a myelin/oligodendrocyte glycoprotein. Am J Pathol 1988;130:443-454.
17. Peschl P, Schanda K, Zeka B, et al. Human antibodies against the myelin oligodendrocyte glycoprotein can cause complement-dependent demyelination. J Neuroinflammation 2017;14:208.